Spring 5-1-2011

Design and Calibration of a Wind Tunnel Facility for the Study of Active Flow Control on Wind Turbine Blades

Christopher Paul Walter

Design and Calibration of a Wind Tunnel Facility for the Study of Active Flow Control on Wind Turbine Blades

A Capstone Project Submitted in Partial Fulfillment of the Requirements of the Renée Crown University Honors Program at Syracuse University

Christopher Paul Walter

Candidate for B.S Degree in Mechanical Engineering

and Renée Crown University Honors

May 2011

Honors Capstone Project in Mechanical Engineering

Capstone Project Advisor: _____

Professor Mark N Glauser

Honors Reader: _____

Professor Frederick J Carranti

Honors Director: _____

James Spencer, Interim Director

Date: _____

Abstract

Our group at Syracuse University has been working under Professor Mark Glauser as part of a wind consortium with the University of Minnesota and United Technologies Research Group. Our component of this project will be to develop a system which can be imbedded in an airfoil which can increase the efficiency of the airfoil. Along with developing this "intelligent blade," we will also be characterizing the affect our control system will have on aerodynamic noise. To accomplish these goals, Syracuse University's anechoic jet facility was remodeled to incorporate a wind tunnel within which we could run our experiments. Upon the completion of the facility, calibration experiments were performed on the measurement devices which we are using in during our testing of the airfoil. Calibration data was collected from the force balance, upon which the airfoil is mounted, the pressure transducers which are embedded inside the airfoil. Still to be collected are the sound characteristics of our chamber when the facility is running. For the control system which we will be using to improve the airfoils efficiency, we are referencing past work done by Syracuse University Ph. D. students who have developed control systems and algorithms in the past.

Table of Contents

ACKNOWLEDGMENTS

I would like to thank the Renée Crown Honors Program for their support in this endeavor. I am also very grateful to Professor Mark Glauser for his advisement and help in editing this work as well as Professor Frederick Carranti for his part as Honors Reader. Finally I would like to thank Guannan Wang and Jakub Walczak. It was a great experience working with you and I learned a great deal from my time on this project.

TABLE OF FIGURES

NOMENCLATURE

A	Circular cross-sectional area covered by the wind turbine
A_{cv}	Circular cross-sectional area inside the control volume
A_p	Planform area of an airfoil
A_1	Circular cross-section of lower velocity air after wind turbine
a	Axial induction factor
C_D	Coefficient of drag
C_L	Coefficient of lift
C_p	Coefficient of power
L	Characteristic length of an airfoil
$\dot{m}$	Mass flow rate of air
$\dot{m}_{side}$	Mass flow rate of air through the side of a control volume
P	Power
P_{max}	Maximum theoretical available power
ρ	Density of air
q	Dynamic pressure (Pascal)
Re	Reynolds Number
R_x	Unknown resistor value
R_1, R_2, R_3	Known resistor values
T	Thrust
u	Velocity of air at the wind turbine
u_1	Velocity of air after the wind turbine
V_{AB}	Voltage between point A and B
V_s	Source voltage
V_0	Velocity of air far in front of the wind turbine
v	Kinematic viscosity
Acronyms	
AFC	Active flow control
CFD	Computational Fluid Dynamics
COE	Cost of Energy
MW	Megawatts
NREL	National Renewable Energy Laboratory
O&M	Operations and Maintenance

I. Historical Overview

In today's society, it is becoming increasingly important for society to be conscious of the effects of using nonrenewable forms of energy production. This awareness has caused an ever increasing interest in renewable forms of energy and improving on those techniques that are already in use today. These methods include the harnessing of natural forces such as energy from wind and wave. Wind energy harvesting in particular has become progressively more popular and the increasing interest stems not only from the environmental advantage, but also some economical ones. The use of wind turbines creates no CO_2 emissions, which proponents of these turbines often point out as their greatest advantage. These turbines also reduce our reliance on fossil fuels, which as we can see from Figure 1, are also responsible for the majority of our CO_2 emissions.

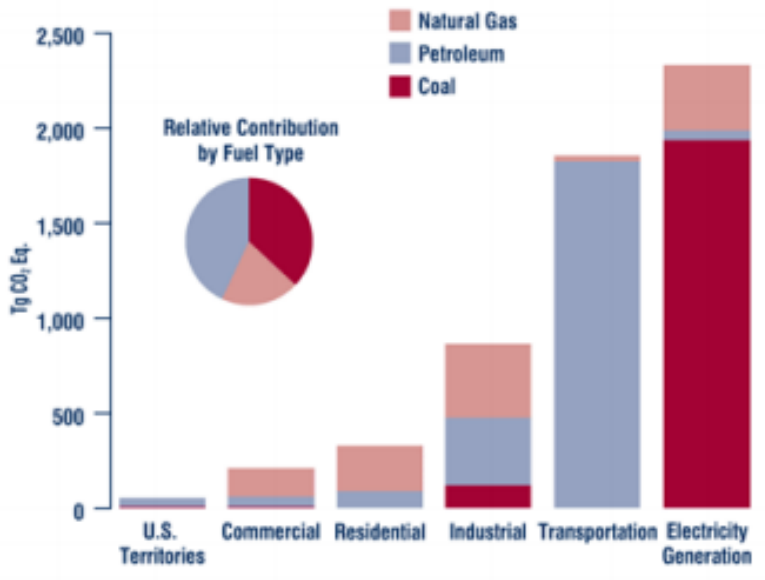

Figure 1 - US Carbon Dioxide Emissions [1]

Another reason to be looking for supplementary sources of energy is to become less dependent on foreign countries for our energy. As we move away from our widespread use of petroleum, wind and other renewable forms of energy are going to become more and more popular sources of energy in the US and other countries. With the use of wind energy there will also be an increase in job creation, which can be a great advantage with our current economic situation and for the future.

At the start of 2010, the wind turbines installed in the United States had the capacity to generate a combined 40,000 MW of power and provided about 3% of the power in the US [2]. As wind power is increasing in popularity it is necessary to carry on advancing the technology so that it can continue to stay an economically competitive choice for power generation. To do this, we refer to the cost of energy, which is calculated using the following equation:

$$COE = \frac{Lifetime\ Energy\ Capture}{Capital\ Cost + Operations\ \&\ Maintenance}$$

Equation 1 – Cost of Energy Equation [2]

From equation 1, we see that the COE can be decreased by lowering the cost of O&M and materials or by creating more reliable wind turbines that require less maintenance. Another approach would be to increase the possible power output of the turbines by either making them larger or improving their efficiency. Our goal in this research will be to lower the COE using this second strategy.

II. Power Generation of Wind Turbines

The power generated by wind turbines comes from the conversion of kinetic energy to mechanical energy and then to electrical energy. Since it is not possible to remove all of the kinetic energy from wind, the actual power we can obtain will be less than the theoretical available power. The ratio of these two values is denoted by C_p, the coefficient of power. The limit is known as the Betz limit and states that the maximum C_p that can be achieved is 16/27 or 0.593 [3].

This limit was theorized based on an ideal wind turbine with a frictionless 1-D disc as a rotor. To start, we apply the axial momentum equation over this rotor using the control volume shown in Figure 2.

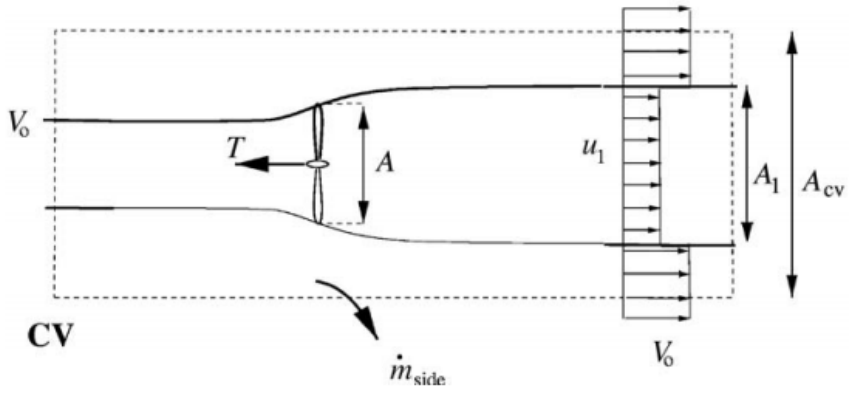

Figure 2 - Circular Control Volume over a Turbine [3]

Simplifying based on the fact that we are doing this over an ideal turbine, we get

$$\rho u_1^2 \mathrm{A}_1 + \rho \mathrm{V}_0^2(\mathrm{A}_{\mathrm{cv}} - \mathrm{A}_1) + \dot{\mathrm{m}}_{\mathrm{side}} \mathrm{V}_0 - \rho \mathrm{V}_0^2 \mathrm{A}_{\mathrm{cv}} = -\mathrm{T}$$

Equation 2 – Axial Momentum Equation over an Ideal Turbine [3]

Using conservation of mass, we can then simplify this argument to get the value of $\dot{\mathrm{m}}_{\mathrm{side}}$ and $\dot{\mathrm{m}}$ whose expressions are

$$\dot{\mathrm{m}}_{\mathrm{side}} = \rho A_1 (\mathrm{V}_0 - u_1)$$

$$\dot{m} = \rho A_1 u_1$$

Equations 3 and 4 – Mass Flow Rates over the Turbine and Out of the Control Volume Sides [3]

Substituting these equations into equation 3 and solving for the thrust yields

$$T = \dot{m}(V_0 - u_1)$$

Equation 5 – Thrust of the Air over a Turbine [3]

The power for our ideal turbine can be found using the kinetic energy equation on our control volume (Figure 2)

$$P = \frac{1}{2}\rho u_1 A\left({V_0}^2 - {u_1}^2\right)$$

Equation 6 – Power over a Turbine [3]

With the addition of an axial induction factor, "a", we can solve for the available power just in terms of the velocity over the turbine, which matches the maximum power we had found before based on the kinetic energy.

$$a = 1 - \frac{u_1}{V_0}$$

$$P_{max} = \frac{1}{2}\rho A {V_0}^3$$

Equations 7 and 8 – Axial Induction Factor and the Available Power [3]

This axial induction factor is a ratio of the wind velocity after the turbine to the wind velocity before the turbine. The maximum energy that can be gained based on the kinetic energy of the two flows has been found to occur when this axial induction factor is equal to 1/3. Knowing the value of a, we can place this value into a differentiated form of the power equation using kinetic energy.

$$P_{max} = \frac{1}{2}\rho A {V_0}^3 (1 - (a)^2 + (a) - (a)^3) = \frac{1}{2}\rho A {V_0}^3 \left(\frac{16}{27}\right)$$

Equation 9 – Axial Induction Factor and the Available Power [3]

In equation 9, the last term represents the maximum coefficient of power that we can obtain. This has become known as the Betz limit and shows the power

that an optimal wind turbine would be able to generate. Modern wind turbines are able to achieve coefficients of performance of up to .5 [3].

III. Current Problems with Wind Turbines and their Solutions

As part of our current project, the University of Minnesota has taken a numerical approach to studying the flow that wind turbines would experience in a wind farm. Their CFD results below demonstrate the major problems with how wind turbines are currently designed and implemented.

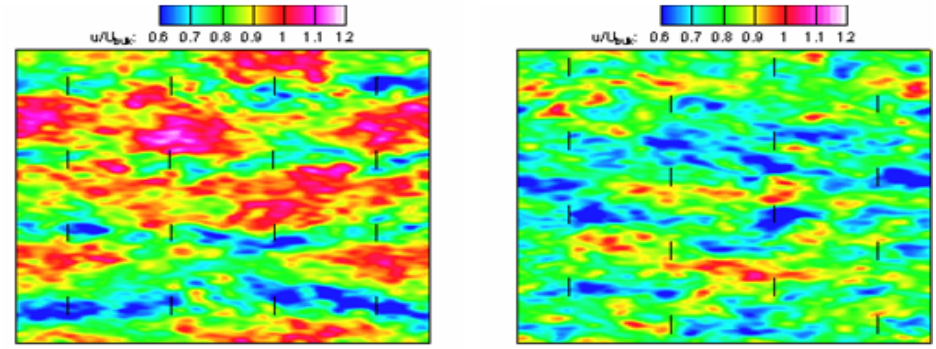

Figure 3 - Instantaneous Streamwise Velocity at Hub Height (Wind Turbines are Indicated by the Black, Vertical Lines) [4]

Figure 3 illustrates two simulated images of the instantaneous streamwise velocity (flowing left to right) at hub height in two different wind farms. The difference between the two is how the wind turbines are arranged, the left image being with the turbines aligned in rows and the right image having them offset from each other. These images demonstrate the large unsteadiness in the flows the wind turbines are experiencing. Neither case shows a steady even velocity field for which many turbines are currently being designed. These images reveal two of the current problems with wind turbine designs and implementation; flow unsteadiness and spatial velocity gradient.

Wind turbines are presently designed for a set operating point where

wind speed and directions are assumed constant. These operating points are selected by performing long-term studies of the wind patterns in a certain area and using the average wind speed and direction. This presents a problem because the majority of the time the wind is not actually at this speed as it comes in gusts and with different intensities. With a set design point, wind turbines cannot fully take advantage of the wind in a given area. Additionally, wind speeds will always vary vertically across the turbine blades because of the Earth's surface boundary layer. In this layer, shear forces from the atmosphere moving over the Earth's surface cause the air velocity near the Earth's surface to be reduced due to the "no-slip" boundary condition imposed at the surface, which causes the wind velocity to go to zero at the Earth's surface.

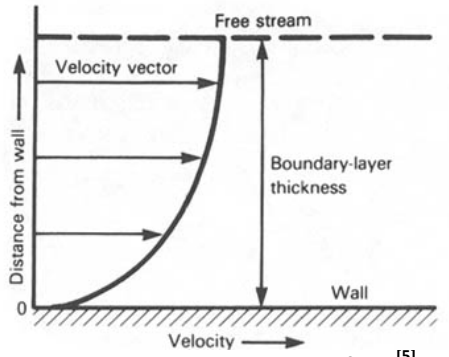

Figure 4 - Boundary Layer along a Surface [5]

Figure 4 illustrates how the velocity profile of a boundary layer will typically look. Since the blades on ground based turbines will always be in the boundary layer, the vertical velocity profile that the blades will see will never be uniform but will always contain wind shear.

A second shortcoming of present wind turbine design deals with the effects of placing them in large wind farms where there are many wind turbines

located in a large open area and all are attempting to use the same wind to generate power. This is problematic because the turbines upstream will generate a great deal of unsteadiness and disruptions in the wind for the turbines that are further down wind as seen in Figure 5:

Figure 5 - Horns Rev Wind Farm, Denmark [6]

As we can see, even if the upstream turbines received consistent optimal wind conditions for their design point, the turbines behind them would not. This turbulence not only reduces the power generated by all of the turbines that are not in the front line but also can cause excessive wear and damage to those turbines that the flow interacts with. Figure 6 makes it quite clear that these turbines would not be seeing a clean boundary layer such as the one in Figure 4, but that the shear they would experience would be much more turbulent, varying both temporally and spatially in 3D.

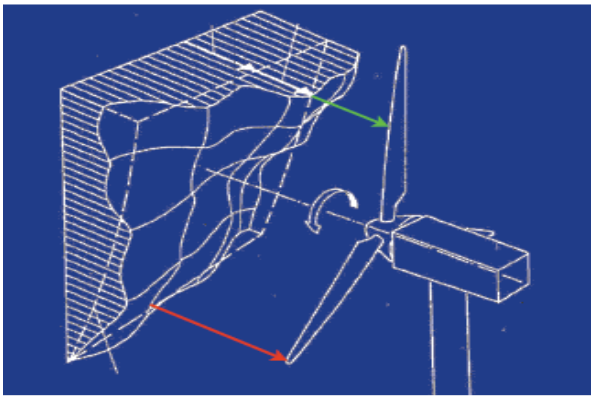

Figure 6 - Wind Shear over a Wind Turbine

The current solution to these two problems is variable active/passive blade pitch control which can be adjusted for changes in larger scale off-design conditions. The problems with using just these techniques are that they have a slow response time and that the changes affect the entire blade [6]. This solution does not take into account local variations in wind along the blade and therefore is not adequate to harvest the full potential power from the wind. In order to account for these variations along the blade length, a control system that is not on the scale of the entire turbine, but can actuate specific locations along each blade based on the local wind characteristics needs to be developed. Not only would this "intelligent blade" system help deal with the problem of varying wind speed depending on the height above the ground, but it can also be used to combat the problem of interference in large wind farms, as well as to reduce blade fatigue.

IV. Active Flow Control and how it Works

There are a large number of AFC devices that are either being proposed or used in modern wind turbines. A few of these will be discussed in this paper including flaps, stall strips and plasma actuators. Trailing-edge flaps have been used for a long time in aircraft control, and their uses for aerodynamic braking and power regulation was studied by NREL in the 1990's [7]. They were found to be useful in power regulation and also in reducing the bending moments at the flap root during turbulence. The problem with adapting these systems from aircraft to wind turbines will be that they are large and complex and have a

relatively slow response time. Power requirements and their noise generation are other drawbacks to trailing-edge flap systems [7]. An improvement over trailing-edge flaps are what are termed “nontraditional trailing-edge” flaps. These flaps function in similar ways to the trailing-edge flaps but they use newer technology to actuate the flaps, which minimizes their drag. The problem with these systems is that they can be unreliable, especially when scaled from model size to full wind turbine size. They also require a high voltage to drive some of the actuation [7].

Using microflaps is another method of trailing-edge active control which has been found to increase lift on an airfoil. They have a faster initial response time because of their trailing-edge location, but this also causes the airfoil to act more like a bluff-body which causes vortex shedding. These vortices can cause added noise which is one of the drawbacks of this method of control along with the fact that it is also a relatively complex system to implement [7]. The active stall strip is an easier system to install and though it can increase the lift to drag ratio, it cannot increase the coefficient of lift for an airfoil. Other operational concerns are the mounting locations of these strips, though more study is needed to fully determine the ideal locations and sizes for these strips [7].

Plasma actuators have also been studied for use on controlling separation over a wing. These actuators function by using a high voltage flowing between two electrodes to create what is known as an “ionic wind.” This “ionic wind” interacts with the boundary layer and delays separation along the airfoil.

These systems are relatively simple in that they have no moving parts and also convert electrical energy directly to kinetic energy, but they are quite inefficient and the current technology does not provide high performance at higher wind speeds where many of the other methods of AFC are more effective [7].

Another method of AFC which Syracuse University has been involved in researching for other applications is synthetic jets. These devices are designed with a diaphragm which oscillates in and out and causes the fluid which is flowing over the surface of the airfoil to be drawn in and then pushed out. These systems are relatively easy to implement and have low power requirements, but due to the fact that they have a cavity, they are very susceptible to dust, ice and other foreign objects corrupting the jet and degrading performance [7].

The final method of AFC that will be discussed in this paper will be blowing and suction, which will also be the method our group will be studying in our future experiments. The basic function of these devices is to increase the amount of higher momentum fluid which is in contact with the surface of the wing, therein delaying separation of the flow. Blowing does this by adding high-momentum fluid into the flow while suction removes the low-momentum air along the surface allowing the higher momentum air above it to come closer to the surface [7]. The blowing or suction normally occurs through slots, which are located along the span of the surface and can be located anywhere along the chord. The benefits of these systems are that they have been successfully used in aircraft applications, though because they require a large compressed air

storage/generation system, they would take up more interior space then some of the other methods discussed above. Also, the spanwise slots that are needed for this method of actuation can be quite complex [7].

The current focus of research for a number of groups including ours is on the development of this "intelligent blade" system which will use a combination of control to increase the power output of turbines [8]. AFC is a general term, but in the context of our research AFC will refer specifically to controlling the separation of the flow over the surface of our airfoil. In the case of a wind turbine, the AFC will be employed to delay the flow separating from the surface of the blade as α is increased. As α is increased, the velocity of the flow on the top of the airfoil increases compared to the velocity along the bottom. This results in the pressure below the airfoil being higher than that above and consequently a resulting "lift" force which is perpendicular to the flow. Since increasing α is also increasing the surface area that is exposed to the flow, it also increases the "pressure drag" on the flow or the force that is parallel to flow. As α is increased further, it reaches a point where the flow will separate from the surface of the wing or turbine blade as shown in figure 7. Seperation of the flow can happen with both turbulent and laminar flows over an airfoil.

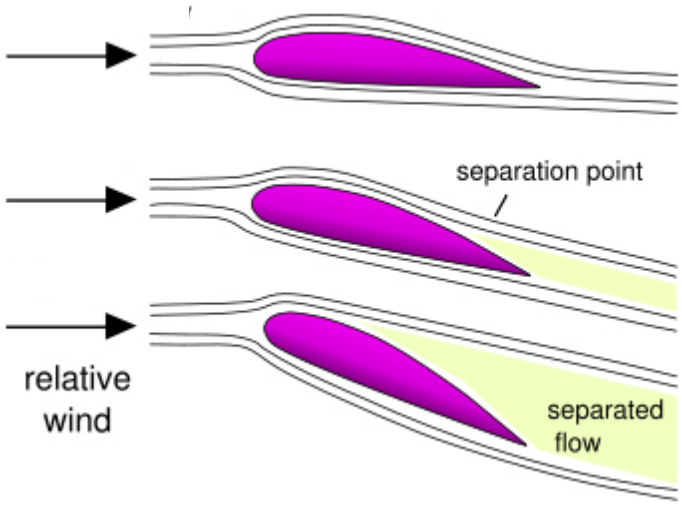

Figure 7 –Steady Flow (top), Stall Point (Middle) and Separated Flow (Bottom) Over a Wing [9]

Figure 7 illustrates a laminar flow over a wing section, as α is increased, the wing will reach a stall point (middle case) at which point any additional increase of α will result in a reduction of lift and a great increase in drag. This is because as the separation point moves up the wing from the trailing edge towards the leading edge, a turbulent flow is in contact with the wing after the separation point, which is the cause of the increase in pressure drag on the surface.

V. Our Approach of Active Flow Control

To delay this separation of flow, a combination of sensors and actuators will be embedded in our airfoil. The sensors will measure the pressure at points along both the top and bottom surfaces of our airfoil at the midspan. These sensors, will allow us to determine when separation is occurring along the airfoil. Actuation will then be used in the form of blowing slots to prevent this separation. The fluid being blown into the flow will be pressurized air blown from slots controlled by Parker Gold Ring solenoid actuated valves. These valves

have an orifice diameter of 1/8 inch and require power from a 24V DC source. A control algorithm will be developed which determines the correct actuation that should occur when certain events are determined by the pressure signals. This method of flow control will not only lessen unwanted separation caused by turbulence and disturbances that the wind turbine experiences but will also help the blade be more efficient at varying wind speeds when combined with the other full blade control systems mentioned above [8].

VI. Past Experiments and Simulations

This method of active control has been chosen based on a number of past experiments performed at Syracuse University. A simulation has also been done as a precursor to this project to determine what kinds of improvements in power we could expect. One of these past experiments was performed at Syracuse University by Pinier et al. using a NACA - 4412 airfoil [10]. They developed a closed loop control system on the NACA - 4412 airfoil using embedded pressure sensors and piezoceramic synthetic jets [10]. What they found with their control system was that they could not only delay flow separation but that their closed loop system required less actuation than an open loop system would need, as shown in figure 8.

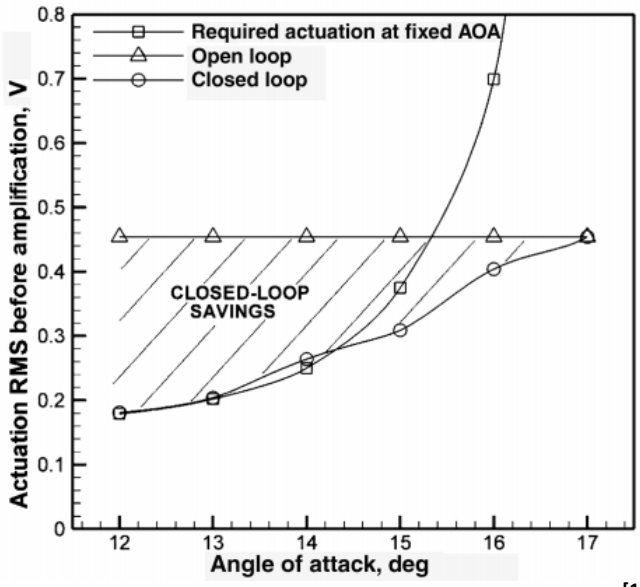

Figure 8 - Savings with Closed-Loop vs. Open Loop Control [10]

The relevance of these findings to our experiments is that they were able to demonstrate a closed loop control system which controlled flow separation using only surface pressure data. This research also demonstrates that it is "critical to keep the control active and the flow attached at all times to achieve the control objective without excessive power need" [10]. These developed control algorithms will be used in the development of our own simple proportional feedback loop for our airfoil [8].

Knowing that closed loop flow control could delay flow separation, the SU team performed an initial Blade Element Momentum Method (BEM) [3] analysis on a NREL S809 airfoil to estimate the benefits that a separation delay of 5 degrees would yield. After optimizing the blade profile shape a comparison was made between the coefficient of lift and the coefficient of drag of the blade with and without flow control. Figure 9 shows these coefficients vs. α and the

effect of the flow control.

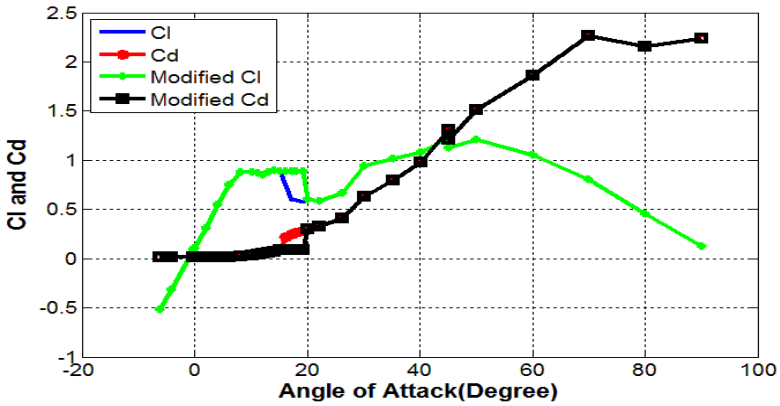

Figure 9 – Coefficients of Lift and Drag vs. AoA with and without Delayed Separation [11] [8]

The advantage from this delay in separation is its effect on the overall power output of the turbine. A theoretical turbine using this control would see a large increase in potential overall power output, (figure 10) most of which is generated from the outer half of the blade (meaning the half furthest from the hub.)

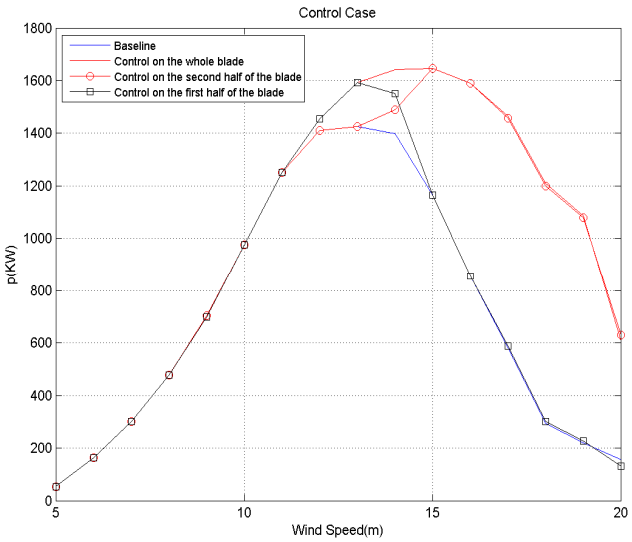

Figure 10 - Potential Power Output with Control from BEM Calculation [7]

VII. Facility

These experiments are being performed in Syracuse University's anechoic wind tunnel located at the Skytop Facility.

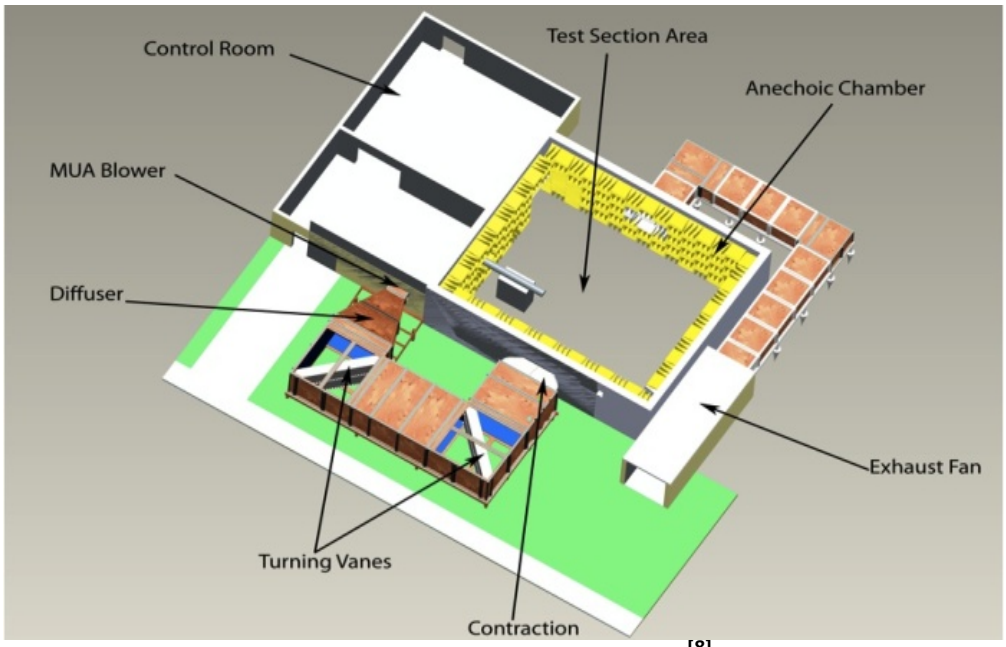

Figure 11 - 3D Model of Skytop Research Facility [8]

The facility consists of an open loop wind tunnel that has been built through an existing anechoic chamber (see Figure 11.) The original facility is used to test flow control on a jet while the new path has been constructed to facilitate our study of flow control over wind turbine blades. The test section for these experiments will be 1 x 1m and we currently have a flow velocity of about 7 m/s which was determined through the use of a Pitot tube (figure 12.)

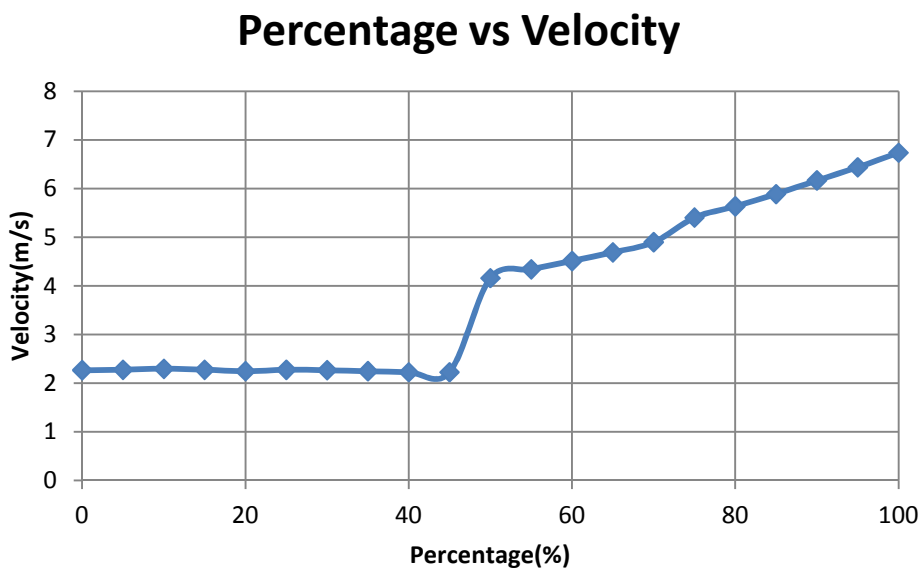

Figure 12 - MUA Percentage of Flow vs. Measured Wind Speed at Test Section [8]

The test section is in a 26ft x 20ft x 14ft anechoic chamber whose walls, ceiling and floor are made from reinforced 12in thick single pour concrete. The interior of the chamber is covered with fiberglass wedges which have a cutoff frequency of 150Hz. The flow through the tunnel is processed by both a Make-Up Air (MUA) unit capable of supplying 7kSCFM (standard cubic feet per minute) to 14kSCFM of air at temperatures up to 90°F and an Eductor fan which will reduce pressure build up in the chamber as the wind tunnel is running.

The construction of the tunnel started with the laying of large concrete blocks for a base, into which 4 x 4 in posts were fastened. On top of this, a platform of 2 x 4 in and 2 x 10 in beams was constructed. This platform was covered in plywood sheets and became the inside floor of our tunnel. The walls of the tunnel were created using 2 x 4 in beam frame with a plywood sheet used for the inside surface. After the wooden framework was assembled, the tunnel

was weather-proofed using a metal siding which covers all of the outside walls of both the settling chamber and the wind tunnel. The roof was weatherproofed with an asphalt roofing material and flashing was added in some locations to prevent unwanted pooling of water. After the completion of the exterior protection of the tunnel, the interior of the tunnel was covered in a layer of 1" thick (two layers were used in the settling chamber) Linacoustic material to help dampen outside sounds and to insulate the flow from outside conditions.

The flow starts from the MUA located on the roof of the building and is directed down and turned 90 degrees into the diffuser. The diffuser opens into an 8 x 8 ft settling chamber which has two sets of turning vanes to prevent large losses in flow velocity in the corners as the flow is turned 180 degrees. The flow then passes through a honeycomb material in order to straighten the flow and two screens whose purpose is to even the flow velocity. Immediately following the screens is a contraction which brings the cross section of the flow from 8 x 8 ft to 1 x 1 m. It is right after this contraction that the flow enters the anechoic chamber and is directed to the test section through a 1 x 1 m straight section. After passing through the test section, the majority of the flow is caught with a catcher and is brought back to a 4 x 4 ft cross section and then directed to the exhaust fan.

The affect that our flow control will have on the acoustics of wind turbines is also of interest in our group's research. To understand where to place our acoustic measurement devices, we needed to determine the origins of noise

from a wing. For our experiments there are three main sources of noise. The first of these is our test section, which acts as a low Mach number jet. In order to find the noise characteristics of this flow, the Lighthill equation is used as a basis.

$$\frac{\partial^2 \rho}{\partial t^2} - c_0^2 \frac{\partial^2 \rho}{\partial x_i^2} = \frac{\partial^2 T_{ij}}{\partial x_i \partial x_j} - \frac{\partial f_i}{\partial x_i}$$

Equation 10 - Lighthill Equation for Low Mach Number Jet [13]

$$T_{ij} = \rho_t u_{ti} u_{tj} - \tau_{ij} + \left(p - c_0^2 \rho\right) \delta_{ij}.$$

Equation 11 - The Lighthill Stress Tensor [13]

This equation shows sound sources as the difference between the acoustical approximations and the exact equations of wave motion. With the assumption that this is a low Mach number flow, we can presume the flow is about isentropic and the jet is a compact jet meaning that the diameter of the jet is much smaller than the wavelength of the sound, we get the following sound characteristics for a low Mach number flow jet.

$$\frac{\overline{p^2}}{\left(\rho_0 c_0^2\right)^2} \sim \left(\frac{D}{r}\right)^2 M^8$$

Equation 12 - Characteristic Sound Equation from a Low Mach Number Jet [13]

In Equation 12, p is the pressure of the flow, D is the diameter of the jet, r is the distance from the source to the observer and M is the Mach number of the jet. The ρ_0 and c_0 are the density and the speed of sound of the flow at the observer's location, respectively.

The second source of sound from our experimental setup will be from the

airfoil itself due to its solid surfaces. What we find from these surfaces is a dipole sound structure with maximum noise generated in the cross-flow direction [13]. This noise will again depend on p, the pressure of the flow; a characteristic surface length of the airfoil, D; the distance from source to observer, r and the Mach number of the flow, M. P_0 and c_0 are the density and the speed of sound of the flow at the observer's location as with the jet noise discussed above.

$$\frac{\overline{p^2}}{\left(\rho_0 c_0^2\right)^2} \sim \left(\frac{D}{r}\right)^2 M^6$$

Equation 13 – Characteristic Sound Equation of a Compact Body in a Turbulent Flow [13]

Equation 13 shows us that from a compact body the sound is proportional to the Mach number to the sixth power and not the eighth power as with the jet noise discussed above.

The final location of noise generation from our experimental airfoil will be the aerodynamic sound produced by an edge. In our experiments, the main cause of this type of noise will be the trailing edge of the airfoil. The characteristic equation of this edge sound is

$$\frac{\overline{p^2}}{\left(\rho_0 c_0^2\right)^2} \sim M^5 \left(\frac{l}{r_e}\right)^3 \left(\frac{l}{r}\right)^2$$

Equation 13 - Characteristic Sound Equation of an Edge [13]

Equation 14 shows that the edge sound scales with the fifth power of the flow speed. Also this demonstrates that edge noise is the dominant factor in turbulent flow as the r_e^{-3} term indicates eddies close to the edge are the only

contributors to emanated sound [13].

Figure 13 illustrates the flow speed dependence of trailing edge noise. The left distribution applies to situations where eddies impacting the airfoil are much larger than the chord length of the airfoil and the right distribution applies when eddies are smaller in relation to the chord length [13].

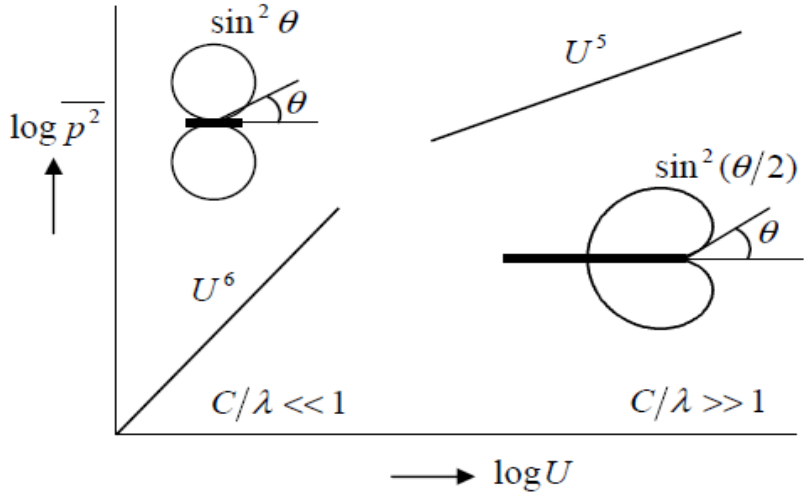

Figure 14 - Directivity of the Sound from an Airfoil [13]

An array of microphones has been set up in the anechoic chamber in order to measure the far-field noise at specific angles using the leading edge of the airfoil at $\alpha = 0^o$ as a reference. These α have been chosen based on figure 14, which shows that the majority of the noise produced by wind turbines emanates from the trailing edge back towards the leading edge. The microphone angles where measurements will be taken are 30^o, 60^o and 90^o from the flow direction as demonstrated in Figure 14 below:

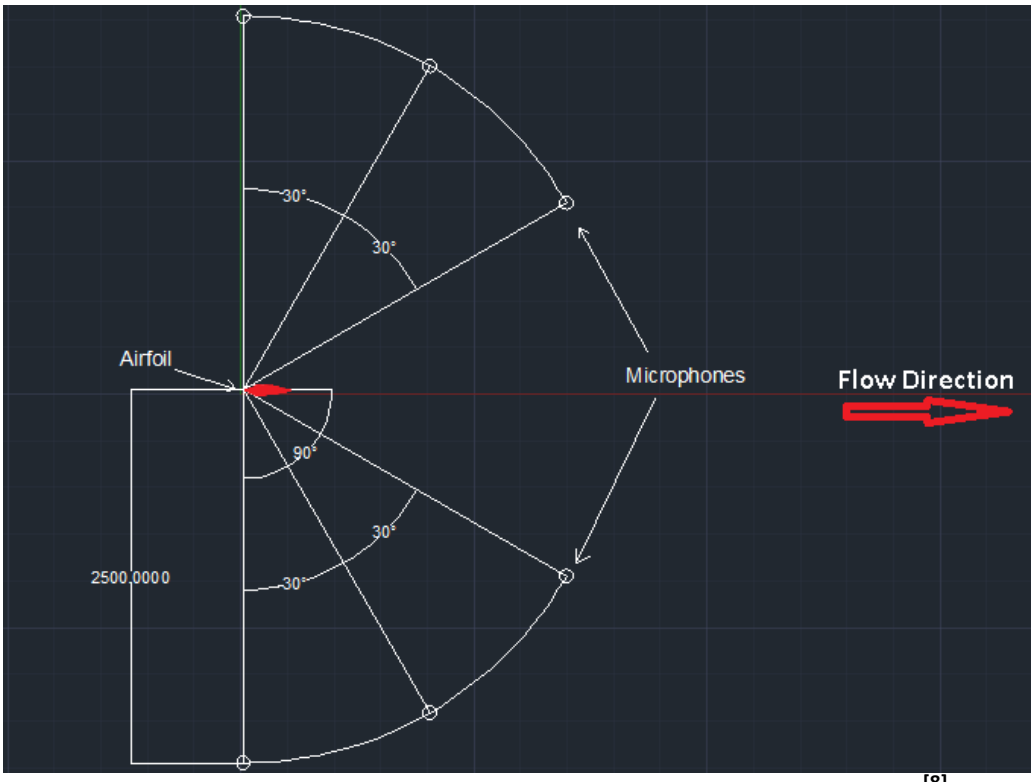

Figure 15 - Diagram of Microphone Orientation Using Airfoil as Reference [8]

The microphones we will be using are 6 G.R.A.S. type 40BE ¼ inch pre-polarized free field condenser microphones with G.R.A.S. type 26CB ¼ inch preamplifiers providing excitation. They have a frequency response and dynamic range of +/- 1dB from 10 Hz - 40 kHz or +/- 2dB from 4 Hz - 100 kHz.

VIII. Airfoil and Mounting

The airfoil we have designed for use in these tests uses a shape which has been specifically developed for wind turbine applications. It is 1 m in length and has a chord length of 250 mm. Our initial model was constructed of laser cut Plexiglas ribs whose shape and size was based on dimensions provided to us by Clipper for the purposes of this research. There were two .5in x .5in aluminum spars that extended from one end of the airfoil and out the other side. These

provide rigidity for the airfoil and also a location to mount the airfoil to the force balance which will be discussed below. The airfoil ribs were covered in a thin balsa sheet which was then covered with a layer of MonoKote to make the airfoil surface as smooth as possible. Eighteen SensorTechnics differential pressure transducers were placed inside of the wing with nine pressure ports along the suction side and nine pressure ports on the pressure side, all evenly spaced and located along the mid span.

The airfoil is mounted with the span oriented vertically on a three component Aerolab pyramidal force balance which will be directly below the entrance of our test section, out of the direct flow. This system will allow us to take direct lift measurements during our experiments. This force balance has an incrementing system that allows adjustment of α to within a tenth of a degree. The output of the force balance is digitized by a NI SCXI-1520 card which is attached in a NI SCXI-1314 card in a NI SCXI-1001 chassis. This SCXI then transfers the data to a PXI-6070 E (Multifunction I/O) port in a PXI-1042 chassis. These signals are collected by VI's which have been written for each experiment using LabView 8.5.

The actual lift measurements from the force balance are taken by a load cell. These load cells consist of a full Wheatstone bridge, which is a common circuit used for load cells. The full Wheatstone circuit contains four resistors oriented as shown in Figure 15 below.

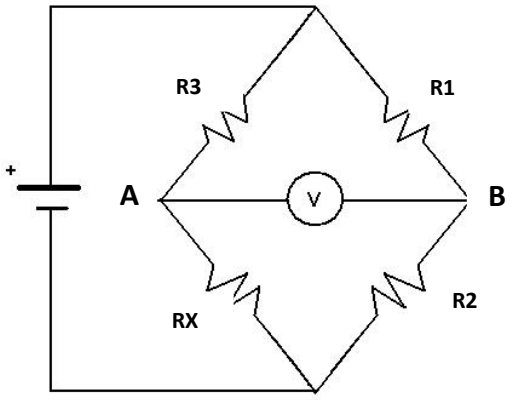

Figure 16 - Diagram of a Full Wheatstone Bridge

The resistors labeled R1, R2 and R3 are chosen based on the size of the voltage being applied and also the resolution of the resistance that was required. Rx in the figure above is proportional to what is being measured; in this case a force. Knowing the voltage applied, the value of the voltage from A to B and the values of the three resistors, the value of Rx can be determined by using Kirchhoff's laws and developing the following relationship:

$$V_{AB} = V_S * \left(\frac{R_X}{R_3 + R_X} - \frac{R_2}{R_1 + R_2}\right)$$

Equation 15 – Voltage between a and B in terms of Source Voltage and Resistances

This relationship tells us that the voltage between A and B has a linear relationship to the resistance caused by the applied load. This knowledge was used to design a simple experiment to determine the function which will convert the voltage output to a force.

IX. Initial Calibrations and Experiments

To perform this calibration, known weights were applied to the force balance and we measured the specific voltage that was output by the load cell.

A wire was secured to the point to which an airfoil would normally be attached and was run over a single pulley and oriented so that it was in line with the direction the load cell measured and was at the same height. At the unsecured end of the wire we placed a carriage of known weight. The voltage output was measured and recorded from the load cell as we added weights accurate to the 1/100th of a pound to the carriage. This data produced the following calibration curve using Microsoft Excel. A best fit line gave us the linear equation relating the voltage output to the loading of the load cell.

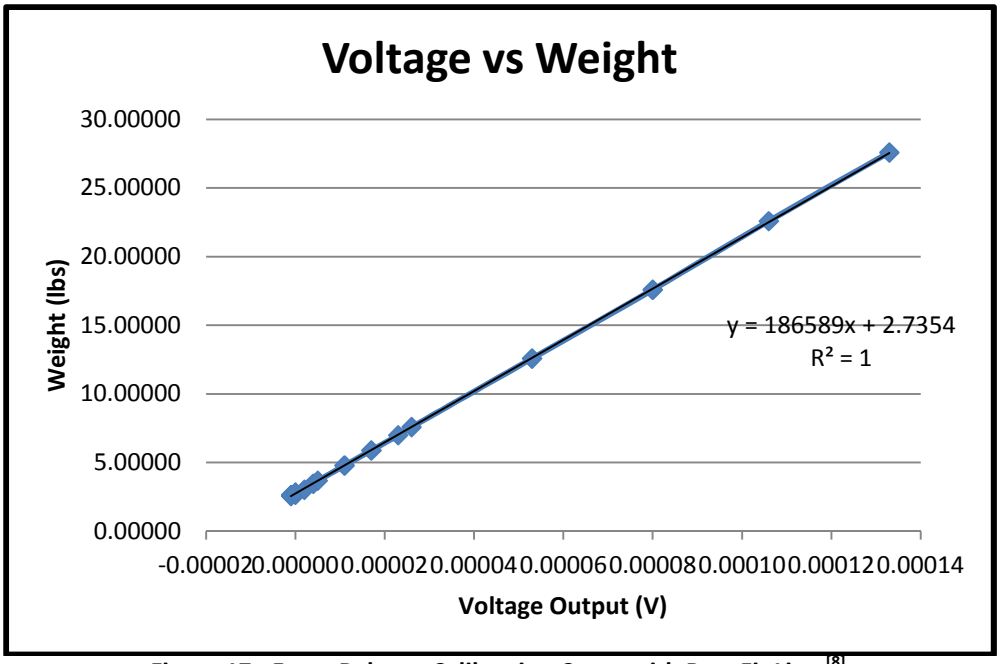

Figure 17 - Force Balance Calibration Curve with Best Fit Line [8]

This equation was written into our VI's in LabView so that we would get an output of force when running experiments. This measurement of lift will be compared to an integration of the pressure data we collect from the pressure transducers in the wing.

With this calibration, we were able to run an initial test of our

airfoil and gather lift measurements from the force balance. Lift measurements were taken at specific AoA and were recorded. Along with Reynolds number calculations, we used these force balance lift force to calculate the C_L at consecutive AoA. The C_L is calculated using equation 17 and is dependent on characteristics of both the flow and the airfoil.

$$C_L = \frac{L}{qA_p}$$

Equation 16 – Coefficient of Lift

These C_L were then plotted with for their corresponding AoA in order to obtain Figure 17.

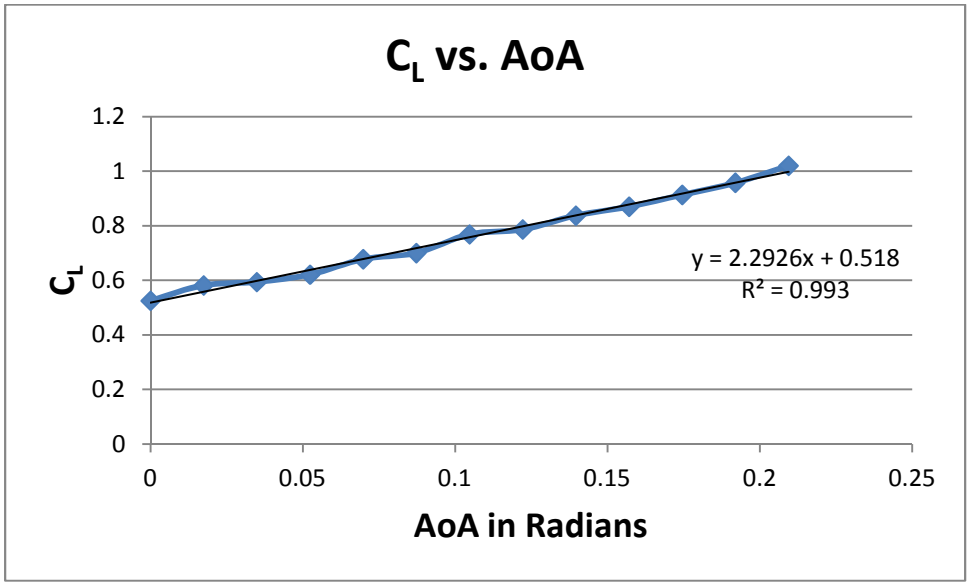

Figure 18 - CL vs. AoA of first Airfoil Design

Figure 17 can be compared to what a standard C_L vs. AoA graph typically looks like in Figure 18.

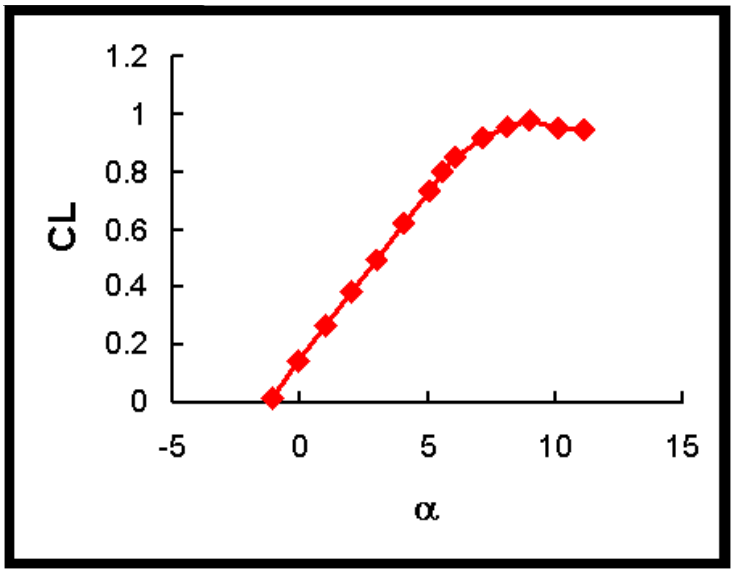

Figure 19 - General CL vs. AoA curve (This information is not readily available for our airfoil) [14]

In comparison, the C_L measured at lower AoA are generally higher on our airfoil than a standard curve, but the C_L also depends on the Reynolds number of the flow.

Data from a pitot tube allowed us to find the Reynolds number of the flow using equation 16.

$$Re = \frac{V_0 L}{\nu}$$

Equation 16 – Reynolds number of a flow

The Reynolds number of the flow allows us to compare this flow to other work done. The Reynolds number of a flow is a dimensionless number which compares the inertial forces to the viscous forces. This number also characterizes the flow as either laminar or turbulent, with the transition Reynolds number around 5×10^5 for most fluids. Two flows with the same Reynolds number can be considered similar, which is important when modeling a flow.

X. Conclusions and Future Work

With the wind tunnel facility completed, we moved on to setting up our initial experiments. While we have been waiting to have a new airfoil manufactured using rapid prototyping through the Bioengineering Department at Syracuse University, we have run some initial tests to demonstrate the validity of our experimental setup. Using calibration data we have been able to find a rough C_L vs. AoA curve which demonstrates some of the behavior that we would expect from a standard curve. We have also taken measurements from our pressure transducers but due to an apparent malfunction in two of the sensors, we were not able to accurately compare an integration of the pressures to the lift we measured from the force balance.

When our new airfoil is completed we will begin assembly, starting with the pressure transducers and the hoses we will need for both the transducers and actuation. When we have assembled the wing, we will place it onto the force balance. Initially, we will be taking simultaneous measurements from the pressure transducers, as well as the force balance, and comparing them. After the calibration and initial tests, we will start with simple proportional feedback loop control using actuation to determine the effect that it has on the flow separation over the wing.

In parallel, we will be placing the microphones into the anechoic chamber and attempting to characterize the chamber. We will be using our preliminary tests results to determine if the acoustic treatments of the surfaces in the

anechoic chamber are adequate, and if not, we will need to add additional treatment. We will also need to determine the noise signatures of the chamber so that the chamber can be characterized for our future experiments.

References

[1] "Carbon Dioxide - Human-Related Sources and Sinks of Carbon Dioxide | Climate Change - Greenhouse Gas Emissions | U.S. EPA." *US Environmental Protection Agency*. Web. 21 Apr. 2011. <http://www.epa.gov/climatechange/emissions/co2_human.html>.

[2] Ryser, Jeffrey (24 January 2011). "Wind power installation slowed in 2010, outlook for 2011 stronger: AWEA". Platts. Retrieved 2011-02-26.

[3] Hansen, Martin O. L. *Aerodynamics of Wind Turbines*. Second ed. London: Earthscan, 2008. Print.

[4] "Large-Eddy Simulations of Wind Farms." EOLOS Consortium. University of Minnesota. 16 May 2011. Lecture.

[5] "SP-4103 Model Research." *NASA History Program Office*. NASA. Web. 21 Apr. 2011. <http://history.nasa.gov/SP-4103/app-f.htm>. Volume 2

[6] "Horns Rev Wind Farm." *ScienceNW*. Web. 16 Apr. 2011. <http://sciencenw.com/winds-turbines-produce-clouds-and-a-loss-of-efficiency/>.

[7] Johnson, Scott J., C. P. "Case" Van Dam, and Dale E. Berg. "Active Load Control Techniques for Wind Turbines." *Sandia Report* SAND2008-4809 (2008): 1-132. Print.

[8] Glauser, Mark N., Guannan Wang, and Jakub M. Walczak. *Benefit of Active Flow Control for Wind Turbine Blades*. Syracuse University Research Group. Web. 2010-2011.

[9] "Forces - Lift - Leroy R. Grumman Cadet Squadron." *Home - Leroy R. Grumman Cadet Squadron*. Web. 16 Apr. 2011. <http://www.cap-ny153.org/forceslift.htm>.

[10] Pinier, Jeremy T., Julie M. Ausseur, Mark N. Glauser, and Hiroshi Higuchi. "Proportional Closed-Loop Feedback Control of Flow Separation." *AIAA Journal* 45.1 (2007): 181-90. Print.

[11] E. Muljadi and C.P. Butterfield, “Pitch-Controlled Variable-Speed Wind Turbine Generation”, NREL, Presented at the 1999 IEEE Industry Applications,Society Annual Meeting, Phoenix, Arizona, October 3-7, 1999.

[12] Tinney, Charles E., Andre Hall, Mark N. Glauser, Lawrence S. Ukeiley, and Tim Coughlin. "Designing an Anechoic Chamber for the Experimental Study of High Speed Heated Jets."*AIAA Journal* 2004.0010 (2004): 1-12. Print.

[13] Oerlemans, S. *Detection of Aeroacoustic Sound Sources on Aircraft and Wind Turbines*. Thesis. Proefschrift Universiteit Twente, Enschede., 2009. Print.

[14] "NASA Quest Aerospace Team Online." *Welcome to NASA Quest!* Web. 26 Apr. 2011. <http://quest.nasa.gov/people/journals/aero/duque/s809exp.html>.

A Non-Technical Summary of this Project

The focus of this project is to develop an aerodynamic system which will help improve the efficiency of wind turbines. Our experiments will be run in the Syracuse University anechoic (a room designed to prevent reflection of sound waves off of all surfaces) wind tunnel located at the Skytop Facility. The existing wind tunnel had been used to study a large axisymmetric jet and the building had to be adapted in order for us to be able to perform our experiments. It took over a year for a group of students (Ph. D, masters and undergraduate) to complete the conversion, which mainly consisted of building a large tunnel system which allowed us to deliver a flow of air to our test section inside the anechoic chamber. The construction was done mainly using 2"x4" beams and 4'x8' sheets of plywood in order to create the tunnel, which had a square cross-sectional area.

With the completion of the facility structure, a great deal of work went into covering the interior surfaces of the tunnel with as acoustic insulation. Not only does this help to preserve the acoustic characteristics of the chamber, but it also prevents the outside environment from having a large affect on our airflow. This mean the insulation will keep the outside temperature from changing the temperature that we have our airflow at. A metal siding was also added to the exterior surfaces of the tunnel which are outside so that the elements would not damage the facility.

With the facility completed, we then built the airfoil which we will be using for some of the preliminary calibration. The size was determined by the dimensions of our test section, which is 1m x 1m, and the shape was provided by Clipper, a wind turbine company who is part of the United Technologies Research Center. (UTRC is part of our research consortium, which also includes University of Minnesota.) This airfoil was a rough model of the airfoil which we will ultimately be using for our experiments and included 18 pressure transducers. These pressure transducers measure what is called differential pressure. This pressure is the difference between atmospheric pressure, and in our case, the pressure along the surface of our airfoil. The importance of these measurements will be discussed later on in this summary.

Meanwhile, the force balance on which the airfoil will be placed needed to be calibrated. To do this, a simple experiment was designed which allowed us to place a known force on the force balance and then read the voltage output. Graphing this data illustrates the linear relationship between the force applied to the balance and the voltage output. We can get an equation from this relationship and use this in later experiments to convert measured voltages directly to forces. In addition to this calibration curve for the force balance, we also preformed a delta function test which gave us the frequency response of the force balance. This information tells us how fast the force balance can sense a change in force.

With the force balance calibrated, we then had to calibrate the pressure transducers to build a curve similar to the one that we made for the force balance. Here the calibration curve illustrates the pressure differential measured by the transducers and its relationship to the voltage that is output by the transducers.

In order to achieve our goal of increased efficiency, we will be implementing a control system into our airfoil. This control system has two basic parts; a sensing part and an actuation part. The sensing part will be the pressure transducers, whose job it will be to sense when the flow of air over our airfoil has begun to separate from the surface. This separation will cause a decrease in the lift, the force from which the power is generated. Basically, this will decrease the power output of the wind turbine.

Along with controlling separation, this system will help with the problem of off design conditions. Modern turbines are designed for the average wind speed of the area where they are to be installed. The problem with this is that for the majority of the time, the wind speed is fluctuating. This causes large variations in power output of turbines. In order to avoid this problem and to smooth the power output, the control system which we are developing can be added. This in combination with existing systems which change the angle of the blade depending on wind speed can improve the power output and allows the turbine to function in wind conditions other than those that they were designed for.

In addition to increasing the efficiency of wind turbines, we are also interested in how our control system will affect the noise given off by a turbine. With modern technology, engineers have reduced the mechanical noise of wind turbines to a negligible amount. What remains is the aerodynamic noise generated from the wind flowing over the wind turbine blades. To measure this noise, we will have 6 microphones set up in an arc around our airfoil. Multiple tests will be run with and without our control system on so that we can determine the difference in noise caused by the control. Studying the noise in correlation with the other data we are able to collect, namely pressure, we will hopefully be able to also make some correlations between how the flow acts and the far-field noise. This will be important because one of the complaints against wind turbines deals with their generated noise. If we can understand the affects of our control on noise, we can be better prepared for correcting this and hopefully reducing wind turbine noise.

The importance of these experiments will be in the improvements in efficiency that our system will add to wind turbines. This will lead to more power at a more consistent rate, hopefully reducing the need for back-up power systems. Our study of noise will ultimately allow us to better understand noise generation from wind turbines and will hopefully allow us to reduce its affects and further improve modern wind turbines.